Published in Environmental science & technology 31, 11, 3180-3187, 1997
which should be used for any reference to this work

^{222}Rn as a Partitioning Tracer To Detect Diesel Fuel Contamination in Aquifers: Laboratory Study and Field Observations

DANIEL HUNKELER,† EDUARD HOEHN,*,‡ PATRICK HÖHENER,† AND JOSEF ZEYER†

Swiss Federal Institute of Technology (ETH), Institute of Terrestrial Ecology, Soil Biology, CH-8952 Schlieren, Switzerland, and EAWAG, Swiss Federal Institute for Environmental Science and Technology, CH-8600 Dübendorf, Switzerland

The use of ^{222}Rn, a naturally occurring radioactive isotope, was investigated as a partitioning tracer to detect and quantify the amount of non-aqueous-phase liquids (NAPLs) in contaminated aquifers. Diesel fuel was chosen as a model NAPL. The diesel fuel−water partition coefficient for ^{222}Rn was 40 ± 2.3, in bottles containing diesel fuel and water at 12 °C. In water-saturated quartz sand contaminated with diesel fuel, the ^{222}Rn emanating from the sand partitioned between diesel fuel and water as expected based on this partition coefficient. In a column containing uncontaminated quartz sand, the ^{222}Rn activity in infiltrated water increased from <0.2 to 4.9 kBq m^{-3}, and in a subsequent column containing diesel fuel-contaminated quartz sand, the ^{222}Rn activity in the water phase decreased to 3.3 kBq m^{-3}. This decrease corresponds to what has been predicted using a mathematical model. At a contaminated field site, the ^{222}Rn activity of groundwater decreased by about 40% between monitoring wells upgradient of the contaminated zone and monitoring wells within the contaminated zone. On the basis of this decrease, the average diesel fuel saturation was estimated using the mathematical model. The calculated diesel fuel saturation was in the range of that found in excavated aquifer material.

Introduction

Contamination of aquifers by non-aqueous-phase liquids (NAPLs) is a common environmental problem. To assess the risk of NAPL contamination and to design appropriate remediation measures, the amount, distribution, and composition of NAPL in an aquifer needs to be known. NAPL contamination is usually located and quantified by analysis of core samples of bore holes. However, laboratory experiments and theoretical considerations have revealed that the volume of core samples is often too small to yield a representative average NAPL saturation (*1*). Partitioning tracer methods may be more accurate because they involve much larger volumes of aquifers (*2*). Furthermore, the same monitoring well can be used for repeated determinations of the NAPL saturation since the methods rely on the quantification of dissolved species and need only water samples.

Partitioning tracer methods were originally developed to determine residual oil saturation in oil reservoirs (*3*, *4*). Recently, the methods have been adapted to locate and quantify NAPL contamination (*2*, *5*, *6*). These methods usually consist of the simultaneous injection of a conservative non-partitioning tracer along with one or several specific partitioning tracers. Partitioning tracers should partition between the NAPL and water phases, but should not be retarded in the absence of NAPL. On the basis of the retardation of the partitioning tracer relative to the non-partitioning tracer, the average NAPL saturation is calculated. The calculation relies on the assumption that a partitioning equilibrium is established between the NAPL and the water phase [local equilibrium assumption (*5*)]. So far, SF_6 (*5*, *6*) and various alcohols (*2*) have been used as partitioning tracers to detect NAPL contamination. The aim of our study was to investigate the feasibility of the use of ^{222}Rn, a naturally occurring radioactive isotope, to detect and quantify NAPL contamination in aquifers.

^{222}Rn is produced by the α-particle decay of ^{226}Ra, an isotope of the natural radioactive decay series of ^{238}U. ^{222}Rn itself decays by an α-particle decay with a half-life of 3.8 days to a series of short-lived daughter products (^{218}Po, ^{214}Pb, ^{214}Bi, ^{214}Po). The ^{222}Rn activity can be determined based on the radioactive decay of ^{222}Rn and its daughter products (*7*, *8*). ^{222}Rn is a chemically inert noble gas; however, it partitions into benzene, toluene, octanol, and other NAPLs (*7*, *9*). Its physical−chemical properties are summarized in Table 1. ^{222}Rn emanates from minerals that contain ^{226}Ra to the surrounding gas or water phase by α-recoil and diffusion (*10*−*13*). Surface waters usually contain little ^{222}Rn since ^{222}Rn is released into the atmosphere. When surface water infiltrates into the subsurface, the ^{222}Rn activity in the infiltrated water increases until a steady state between emanation and radioactive decay is reached (*14*, *15*). The ^{222}Rn activity in the water phase at this steady state is denoted as emanation−decay steady-state ^{222}Rn activity throughout the text. The time necessary to establish the emanation−decay steady-state ^{222}Rn activity is about 5 half-lives (20 days). Hoehn and von Gunten (*14*) used the ingrowth of ^{222}Rn to assess underground residence times of bank infiltration. In their study, ^{222}Rn was transported without retardation in the absence of NAPL contamination, indicating that ^{222}Rn did not sorb to the aquifer matrix. When groundwater, which contains ^{222}Rn at emanation−decay steady-state activity, migrates into a NAPL-contaminated zone of an aquifer, a decrease of the ^{222}Rn activity in the water phase is expected due to the partitioning of ^{222}Rn between water and NAPL. After the groundwater leaves the NAPL-contaminated zone, the ^{222}Rn activity in the water phase is expected to return to the original emanation−decay steady-state value.

In this study, we investigated whether a decrease in the ^{222}Rn activity of groundwater in a NAPL-contaminated zone can be used to detect and quantify the contamination. Diesel fuel was chosen as a model NAPL. The diesel fuel−water partition coefficient was determined in bottles with ^{222}Rn containing water and diesel fuel. The partitioning of ^{222}Rn between diesel fuel and water was studied in batches and columns filled with water-saturated quartz sand from which ^{222}Rn emanated. The aim of the batch experiments was to evaluate whether the partitioning of ^{222}Rn at steady state corresponded to that expected based on the diesel fuel−water partition coefficient despite the continuous emanation and decay of ^{222}Rn. In the column study, the partitioning of ^{222}Rn between diesel fuel and water during advective transport was investigated and compared to the results of a mathematical model that relates NAPL saturation to ^{222}Rn activities. In addition to the laboratory experiments, ^{222}Rn activities were measured in groundwater samples from a diesel fuel-

* Corresponding author telephone: +41-1-823-5525; fax +41-823-5210; e-mail address: hoehn@eawag.ch.
† ETH.
‡ EAWAG.

TABLE 1. Properties of ^{222}Rn

decay constant	3.8 d^{-1}	ref
water solubility[a]	10.8 mM (20 °C)	*9*
K_{ow}	32.4 ± 1.5 (20 °C)	*9*

[a] At 1 atm partial pressure of Rn.

contaminated aquifer to evaluate whether the ^{222}Rn method has the potential to be used to detect and quantify NAPL saturation in the field.

Theory

Processes that govern the transport of partitioning tracers other than ^{222}Rn injected into aquifers have been mathematically described elsewhere (*2*, *16*). These equations do not apply to ^{222}Rn since ^{222}Rn emanates continuously from mineral surfaces and is subject to radioactive decay. Equations were established here that describe the activity of ^{222}Rn in NAPL-contaminated aquifers. The equations rely on the following assumptions: (i) the average distribution of ^{226}Ra, the parent nuclide of ^{222}Rn, in the solid phase is homogeneous on the macroscopic scale (*14*); (ii) the porosity of the aquifer material is constant; (iii) losses of ^{222}Rn from the saturated to the unsaturated zone can be neglected; (iv) the partitioning of ^{222}Rn between the NAPL and water phase is in equilibrium; (v) the partition coefficient is independent of the NAPL saturation; (vi) the NAPL phase is immobile, and (vii) sorption of ^{222}Rn to the matrix is neglected. Based on these assumptions, a one-dimensional mass balance equation for ^{222}Rn was established (eq 1) that takes into account advective and dispersive ^{222}Rn transport, ^{222}Rn emanation from mineral surfaces, ^{222}Rn decay, and partitioning of ^{222}Rn between the NAPL and water phase. The equation was derived in analogy to equations given by van Genuchten and Alves (*17*):

$$\frac{\partial}{\partial t}[(1-S)\theta A + \theta S A^{\mathrm{NAPL}}] = -\frac{\partial}{\partial x}\left[qA - (1-S)\theta D\frac{\partial A}{\partial x}\right] + (1-\theta)\rho P\lambda - [(1-S)\theta A + \theta S A^{\mathrm{NAPL}}]\lambda \quad (1)$$

where t is time (s), x is the flow distance (m), S is the NAPL saturation of pore space (volume of NAPL divided by volume of pore space) (−), θ is the porosity (−), A is the ^{222}Rn activity in water phase at location x at time t (kBq m^{-3}), A^{NAPL} is the ^{222}Rn activity in NAPL phase at location x at time t (kBq m^{-3}), q is the specific discharge of groundwater (m s^{-1}), D is the dispersion coefficient of ^{222}Rn in groundwater (m^2 s^{-1}), ρ is the density of aquifer material (kg m^{-3}), P is the ^{222}Rn emanation rate from mineral surfaces per mass of dry aquifer material (kBq kg^{-1}), and λ is the radioactive decay constant of ^{222}Rn (s^{-1}).

Equation 2 describes the partitioning of ^{222}Rn between the NAPL and the water phase at equilibrium:

$$A^{\mathrm{NAPL}} = KA \quad (2)$$

where K is the NAPL−water partition coefficient of ^{222}Rn (−). Substitution of eq 2 into eq 1 and rearrangement gives

$$\theta[1+S(K-1)]\frac{\partial A}{\partial t} = -\frac{\partial}{\partial x}\left(qA - (1-S)\theta D\frac{\partial A}{\partial x}\right) + (1-\theta)\rho P\lambda - \theta[1+S(K-1)]A\lambda \quad (3)$$

Batch Experiments. For the batch experiments without water flow, q and D in eq 3 can be set to zero, which leads to

$$\theta[1+S(K-1)]\frac{\partial A}{\partial t} = (1-\theta)\rho P\lambda - \theta[1+S(K-1)]A\lambda \quad (4)$$

Solving eq 4 gives

$$A = A_e + (A_0 - A_e)^{-\lambda t} \quad (5)$$

where A_0 is the ^{222}Rn activity in the water phase at $t_0 = 0$. For batches with and without NAPL contamination, respectively, A_e is given by

$$A_e^{S=0} = \frac{(1-\theta)\rho P}{\theta(1+S(K-1))} \quad (6)$$

and

$$A_e^{S>0} = \frac{(1-\theta)\rho P}{\theta} \quad (7)$$

where $A_e^{S>0}$ is the emanation−decay steady-state ^{222}Rn activity in the water phase of batches with NAPL contamination (kBq m^{-3}) and $A_e^{S=0}$ is the emanation−decay steady-state ^{222}Rn activity in the water phase of batches without NAPL contamination (kBq m^{-3}) A approaches $A_e^{S>0}$ or $A_e^{S=0}$, respectively, as t becomes large. Note that $A_e^{S>0}$ is smaller than $A_e^{S=0}$. Dividing eq 7 by eq 6 leads to

$$\frac{A_e^{S=0}}{A_e^{S>0}} = 1 + S(K-1) \quad (8)$$

According to eq 8, $A_e^{S>0}$ is expected to decrease with increasing NAPL saturation S.

Column Experiment. For the flow-through columns, eq 3 was solved neglecting dispersion since transport of dissolved species was assumed to be dominated by advection. If necessary, there is also an analytical solution that includes dispersion (*17*). The following solution of eq 3 is obtained for steady-state conditions ($\partial A/\partial t = 0$):

$$A = A_e + (A_0 - A_e)e^{-\kappa_x x} \quad (9)$$

where κ_x (m^{-1}) is given by

$$\kappa_x = \frac{\theta[1+S(K-1)]}{q}\lambda \quad (10)$$

and A_0 is the ^{222}Rn activity in water phase at x_0 (kBq m^{-3}). A approaches A_e as x becomes large. A_e corresponds to $A_e^{S>0}$ for NAPL-contaminated columns (eq 6) and to $A_e^{S=0}$ for uncontaminated columns (eq 7). While eq 8 can be used to estimate the NAPL saturation based on $A_e^{S>0}$ and $A_e^{S=0}$, eq 9 describes how quickly $A_e^{S>0}$ and $A_e^{S=0}$ are approached. The ^{222}Rn emanation rate P, the density of the aquifer material ρ, and the porosity θ do not have to be known if they are similar in the uncontaminated and the contaminated column.

Experimental Set-up and Field Site

Diesel Fuel−Water Partition Coefficient. The diesel fuel−water partition coefficient for ^{222}Rn was determined in bottles containing tap water and diesel fuel using a method similar to that used for the determination of octanol−water partition coefficients (*18*). Six bottles were filled with tap water. Analysis of tap water before and after filling showed that the ^{222}Rn activity in the tap water remained constant. Afterwards, 18 mL of diesel fuel was added to every other bottle. The bottles were shaken at 12 °C. In bottles without diesel fuel, the ^{222}Rn activity in the water phase was measured at 0, 7, and 31 h after filling; in bottles with diesel fuel, the ^{222}Rn activity was measured at 3, 5, and 24 h after filling. The measurement made after 24 h of shaking confirmed that a partitioning equilibrium had been reached at the earlier sampling times. The intervals between the measurement of the contaminated and the uncontaminated samples were due to the fact that one measurement took approximately 2 h. The measured ^{222}Rn activities were corrected for the time

TABLE 2. Grain Size Distribution of the Quartz Sand

	fractional weight (%)	
grain size (mm)	sand 1[a]	sand 2[b]
0.5−1.0	2.8	3.0
0.25−0.5	73.3	69.2
0.125−0.25	22.9	25.6
0.063−0.125	0.9	2.0
<0.063	0.02	0.01

[a] Used for batch series 1. [b] Used for batch series 2 and columns.

difference between filling of the bottles and measurement. For each bottle with diesel fuel, the ^{222}Rn activity in the diesel fuel phase was calculated from the ^{222}Rn activity in the water phase and the ^{222}Rn activities in the corresponding bottle without diesel fuel. The diesel fuel−water partition coefficient, K, was obtained by dividing the calculated ^{222}Rn activity in the diesel fuel phase by the measured ^{222}Rn activity in the water phase (eq 2). The three values for K were averaged, and the standard uncertainty was calculated.

Batch Experiment. Two batch experiments were performed with the same purified natural quartz sand (Zimmerli/Carlo AG, Zurich, Switzerland) as was used in the ^{222}Rn study of Hoehn et al. (*15*). The grain size distribution of sand no. 1 used for the batch series 1 was slightly different from that of sand no. 2 used for batch series 2 and the column study (Table 2). Since the sand did not contain organic carbon (manufacturers specification), sorption of ^{222}Rn to the sand could be excluded. All experiments were performed at 12 °C, which corresponds to the average groundwater temperature at the investigated field site. Since the moisture content of the aquifer material affects the distribution of NAPLs (*19*) and the aquifer material at the field site was most probably wet at the time of the contamination, the quartz sand was saturated with water before contamination. The water-saturated sand was mixed with diesel fuel (ESSO, Schlieren, Switzerland) for 10 min using an electric mixer. Separatory funnels (2 L) were filled completely with the quartz sand and closed with glass stoppers without any headspace. In each batch series, two separatory funnels were filled with water-saturated uncontaminated quartz sand, and three of them were filled with water-saturated quartz sand contaminated with diesel fuel. The porosity of this sand was determined to be 0.46 ± 0.02, based on the volume of water added to the dry sand and the total volume of the water-saturated sand in the separatory funnels. The high porosity is due to the narrow grain-size distribution of the sand (Table 2) and is in the same as those found in sand columns used by other investigators (e.g., ref 5). From each separatory funnel containing contaminated sand, three samples were taken before filling and three samples were taken after the experiment in order to test the homogeneity of the diesel fuel contamination. The samples were analyzed for total hydrocarbon concentration by IR spectrometry. The separatory funnels were stored at 12 °C for 4 weeks without shaking. According to eq 5, after 4 weeks, the deviation between the actual ^{222}Rn activity and the emanation−decay steady-state ^{222}Rn activity is expected to be less than 1%. After 4 weeks, the water was drained from the separatory funnels into 120-mL vials using a glass tube of 36 cm length and 2 mm inner diameter. The ^{222}Rn activities in these samples were measured using the RAD7 instrument (see below). A sample volume of 50 mL was extracted with CCl_4 to determine dissolved hydrocarbon concentrations (see below). The filled separatory funnels are referred to as batches throughout the text.

Column Experiment. For the column experiment, the same quartz sand was used as was for the batch series 2 (Table 2). The dimensions and operation parameters of the columns are given in Table 3. The size of the columns was chosen based on the minimal sample volume necessary (120 mL) and the required residence time (13 days) of the water in the columns to reach 90% of $A_e^{S=0}$. The columns had a sieve plate at the bottom, which was covered with glass wool, and lateral sampling ports. The sampling ports were fitted with stainless steel hypodermic needles of an inner diameter of 1.6 mm (Unimed, Geneva, Switzerland). Both columns were placed in a vertical position. Column 1 was filled with water-saturated uncontaminated quartz sand; column 2 was filled with quartz sand contaminated with diesel fuel as described for the batch experiment. During the filling of column 2, nine samples of sand were taken from different filling depths and analyzed for total hydrocarbon concentration by IR spectrometry. The columns were connected with steel capillaries and operated with distilled water using a JASCO HPLC pump (JASCO Corporation, Tokyo, Japan). The water contained 10 mM $CaCl_2$ to obtain an ionic strength similar to that at the studied field site. The water flowed first through column 1 (uncontaminated) and then through column 2 (contaminated). The mean residence time of the water, the effective porosity, and the dispersion coefficient were determined by a tracer test with Br^-. NaBr was added to the water at a concentration of 1 mM during 8 weeks. The breakthrough curves were analyzed using the numerical model code CXTFIT2 (*20*). The transport parameters were similar for both columns (Table 3). After 8 weeks of operation, water samples were taken to measure the ^{222}Rn activities. The flow was then stopped for 4 weeks after which time water samples were again taken. At flow conditions, the water samples were taken starting at the column outlet, whereas at no flow conditions, sampling was started at the column inlet to minimize the disturbance. For sampling, a glass syringe of 120-mL volume (Merck, Dietikon, Switzerland) was connected to the steel needles of the sampling ports and allowed to fill within 20 h at a rate of 6 mL h^{-1}. In tests with glass syringes filled with ^{222}Rn-containing water, no losses of ^{222}Rn except for decay could be observed within 30 h. At the sampling port at 10 cm, the ^{222}Rn activity at no flow conditions was not determined because it is likely that the sample would be influenced by water from the column inlet during sampling. The water samples were transferred to 120-mL sampling vials, and the ^{222}Rn activity was immediately measured. The measured ^{222}Rn activities were corrected for decay during the time between sampling and measurement.

TABLE 3. Dimensions and Operation Parameters of Columns

	column 1	column 2
Dimension		
length (cm)	120	
inner diameter (cm)	6.8	
sampling ports at (cm)[a]	0, 10, 30, 60, 90, 120	
Operation Parameters		
temperature (°C)	12	
filling (kg dry weight)	6.7	
flow rate (mL h^{-1})	6.0 ± 0.2	
diesel fuel saturation (%)	0.0	1.4 ± 0.06[b]
effective porosity[c] (−)	0.44 ± 0.02	0.42 ± 0.02
Peclet number[c,d] (−)	1070 ± 50	1100 ± 50
mean residence time[c] (d)	13.2 ± 0.5	12.8 ± 0.5

[a] Samples at 0 cm taken before water entered the column; samples at 120 cm taken at column outlet. [b] Average of nine measurements. [c] From tracer experiment with Br^- as a tracer. [d] Peclet number $Pe = Lv/D$ where L is column length, v, average flow velocity, and D, dispersion coefficient.

Field Site. The field site (Figure 1) is located in central Switzerland, 555 m above sea level, and represents a hydrogeological situation typical for the perialpine belt of Switzerland. The shallow unconfined valley−fill aquifer consists of glaciofluvial outwash deposits (sand and gravel; saturated thickness 2−8 m), which usually contain less than 1.5 ‰ (w/w) organic carbon (*21*). The water table is located 3−4

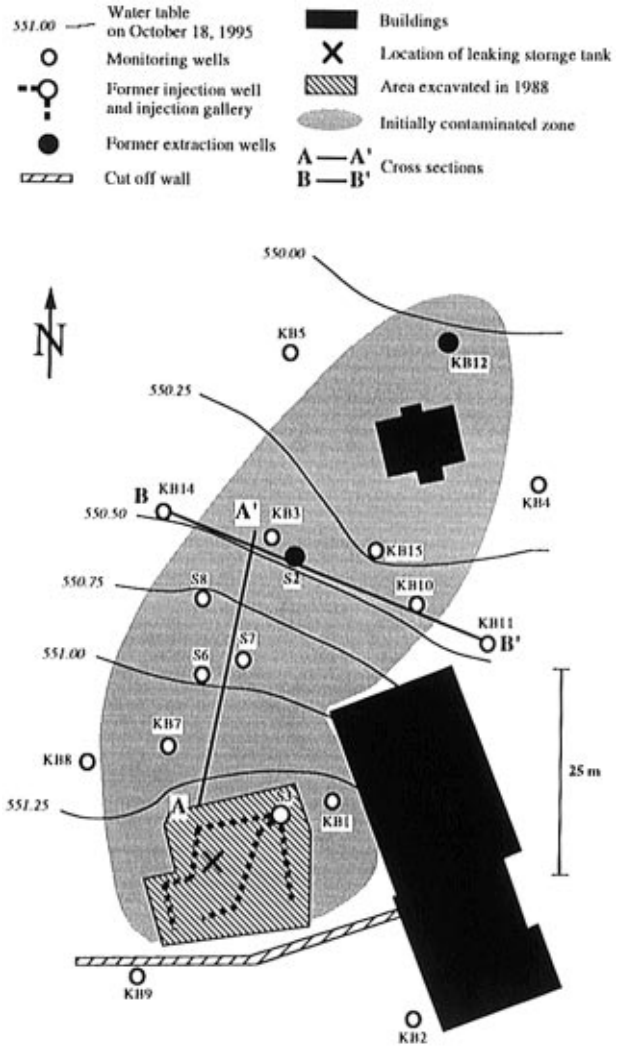

FIGURE 1. Map of field site with water table on October 18, 1995, at natural gradient conditions. Water table contours are interpolations of measurements in monitoring wells.

m below the surface. On the basis of the average hydraulic conductivity (0.5×10^{-3} m s^{-1}), the estimated porosity (0.19), and the hydraulic gradient (2−3%), an average flow velocity of 4.5−7 m d^{-1} at natural gradient flow was calculated using Darcy's law. The average temperature of the groundwater was 12 °C.

The aquifer was contaminated in 1988 by 10−12 m^3 of diesel fuel from a leaking storage tank of a gas station. After discovery of the contamination, contaminated material in the vicinity of the tank (5−10 m) was excavated, floating diesel fuel in free phase was removed by pumping, and an in situ bioremediation scheme was implemented. The initial hydrocarbon concentrations were between 0.9 and 2.5 mg kg^{-1} (S = 1.5−4%) in drilling cores, between 5.5 and 8.6 mg kg^{-1} (S = 9−14%) on the northern boundary of the excavated zone, and up to 72 g kg^{-1} (S = 100%) below the location of the tank. The diesel fuel saturation was calculated assuming a porosity of 0.19 and a density of the aquifer material of 2.5 kg L^{-1}. The field site and remediation measures are described in more detail elsewhere (*22*, *23*). Groundwater samples for ^{222}Rn were taken as described in ref 14.

Analytical Methods

Analysis of ^{222}Rn Activities. In the water samples from the laboratory experiments, ^{222}Rn activities were measured with a Niton RAD7 instrument and a RAD-H_2O attachment (both from Niton Corporation, Bedford, MA). The RAD-H_2O attachment transfers ^{222}Rn from the water sample to the measurement cell by purging ^{222}Rn out of the sample during 5 min in a closed loop filled with air. According to the manufacturer, the stripping efficiency of the ^{222}Rn is 94% for 250-mL sample vials and 99% for 40-mL sample vials. For the 120-mL vials that were used in the laboratory experiments, a stripping efficiency of 97% was assumed. Dissolved hydrocarbons at concentrations measured in the experiments (<3.5 mg L^{-1}) did not influence the efficiency of ^{222}Rn stripping. In the measurement cell of the RAD7, the ^{222}Rn activity is determined after electrostatic collection of α emitters on a solid-state detector based on the ^{218}Po α-decay. After the secular equilibrium between ^{222}Rn and ^{218}Po was established (15 min), the decay of ^{218}Po ($T_{1/2}$ = 3.05 min) was counted four times during 45 min. The detection limit is 0.2 kBq m^{-3} for 120-mL vials. The standard deviation of the measurement is ±10%. In field samples, ^{222}Rn activities were measured by liquid scintillation counting (LSC) except for samples taken on October 29, 1996, for which the Niton RAD7 was used. Filling of the sampling bottles, extraction of ^{222}Rn from the water into a scintillation liquid (toluene basis), measurement of the decay of ^{222}Rn and four daughter products with LSC, and the calculation of the ^{222}Rn activity at the time of sampling is reported in Hoehn and von Gunten (*14*). Instrument signals were converted to ^{222}Rn activities and expressed in kBq m^{-3}. The detection limit of the LSC method is 0.02 kBq m^{-3}. The standard deviation of the measurement is ±20% (*14*).

Analysis of Hydrocarbon Concentrations. To determine the hydrocarbon saturation of the contaminated quartz sand, 20 g of contaminated sand was dried with 8 g of Na_2SO_4 and extracted with 30 mL of CCl_4 by shaking at 250 rpm in a closed flask on a rotary shaker for 48 h at 25 °C. Hydrocarbon concentrations in the extracts were quantified using IR spectrometry and diesel fuel standards (*24*).

For the analysis of dissolved hydrocarbons in field samples, 1-L glass bottles were completely filled and sealed with Teflon-lined covers. To determine concentrations of dissolved hydrocarbons, 400 mL of water was extracted twice with 20 mL of CH_2Cl_2 (B+J Brand High Purity Solvent, Fluka AG, Buchs, Switzerland) containing the surrogate standard *o*-terphenyl. The hydrocarbons were analyzed and quantified with capillary GC as described in Bregnard et al. (*24*). The detection limit was at 0.01 mg L^{-1}. The standard uncertainty was ±20%. The reported uncertainties of all measured values are standard uncertainties determined according to ref 25. Uncertainties of calculated values were estimated using the law of propagation of uncertainty (*25*).

Results and Discussion

Diesel Fuel−Water Partition Coefficient. In bottles containing diesel fuel and water, the diesel fuel−water partition coefficient of ^{222}Rn was determined to be 40 ± 2.3 at 12 °C (n = 3). The diesel fuel−water partition coefficient was similar to the toluene−water partition coefficient, which is 42 at 10 °C (*7*). It was also in the range of the partition coefficients of SF_6 (*5*), which is 32 ± 1.33 for water−trichloroethylene, 24 ± 1.27 for water−dichloromethane, and 45 ± 1.89 for water−*o*-dichlorobenzene.

Batch Experiment. In the batches, the relative standard deviation of the diesel fuel concentration was below 8% (n = 6). This suggests that the distribution of the diesel fuel was quite homogeneous. In both batch series, the ^{222}Rn activity in the water phase decreased with increasing diesel fuel saturation as was expected from eq 8 (Table 4). ^{222}Rn activities in water samples of batches with a similar diesel fuel saturation corresponded within the range of uncertainty. For batches without contamination, the ^{222}Rn activity was higher in batch series 2 than in batch series 1. The higher ^{222}Rn activities in batch series 2 can be explained by the higher fraction of small grains in the sand of batch series 2 (Table 2). The small grains

TABLE 4. Diesel Fuel Saturation and ^{222}Rn Activities of Water Samples from Batches

diesel fuel saturation[a] (%)	^{222}Rn activity in water phase (kBq m^{-3})
Batch Series 1	
0.00	4.13 ± 0.37
0.00	4.03 ± 0.24
0.26 ± 0.02	3.62 ± 0.11
0.51 ± 0.04	3.39 ± 0.12
0.52 ± 0.03	3.28 ± 0.23
Batch Series 2	
0.00	5.49 ± 0.23
0.00	5.61 ± 0.29
1.12 ± 0.08	3.83 ± 0.19
2.37 ± 0.17	2.73 ± 0.11
2.28 ± 0.05	2.71 ± 0.20

[a] Average of six measurements.

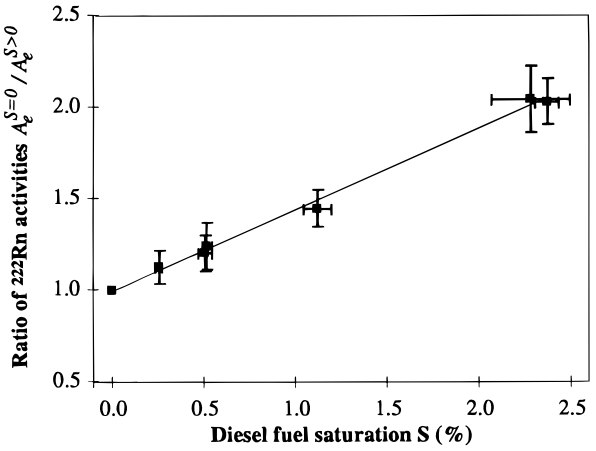

FIGURE 2. Correlation of the ratio of ^{222}Rn activities in water samples from batches without and with diesel fuel contamination vs the diesel fuel saturation. (—) Linear regression; intercept, 1.0; slope, 0.44; R^2 = 0.9966.

release a larger fraction of the ^{222}Rn than large grains due to their higher surface area (*10*). In Figure 2, the ratio of the average ^{222}Rn activity in water from separatory funnels without contamination to the ^{222}Rn activity in water from separatory funnels with contamination ($A_e^{S=0}/A_e^{S>0}$) was plotted as a function of the diesel fuel saturation *S*. A linear dependence of $A_e^{S=0}/A_e^{S>0}$ on *S* was found, suggesting that the partition coefficient of ^{222}Rn is independent of the diesel fuel saturation in the studied range of diesel fuel saturation. Based on the linear relation between $A_e^{S=0}/A_e^{S>0}$ and *S* given by eq 8, the diesel fuel−water partition coefficient K of ^{222}Rn and its standard uncertainty were calculated using linear regression [least square method (*26*)]. A diesel fuel−water partition coefficient of 45 ± 2.0 at 12 °C was obtained for diesel fuel saturation of up to 2.4%. The calculated partition coefficient of ^{222}Rn was similar to the partition coefficient determined in the bottles with tap water and diesel fuel (40 ± 2.3). Thus, the disperse distribution of the diesel fuel in the sand and the continuous ^{222}Rn emanation and radioactive decay did not impair the ^{222}Rn partitioning between the diesel fuel and water.

Column Experiment/No Flow Conditions. At no flow conditions, the ^{222}Rn activity was similar in water samples from all sampling ports of column 1, indicating that the ^{222}Rn emanation was constant throughout the columns (Table 5). Furthermore, the average ^{222}Rn activity in water samples from column 1 (5.46 ± 0.15 kBq m^{-3}) corresponded to the average ^{222}Rn activity in water samples from the uncontaminated batches of batch series 2 (5.55 ± 0.26 kBq m^{-3}; Table 4). In the contaminated column 2, the ^{222}Rn activities were also

TABLE 5. ^{222}Rn Activities in Water Samples at No Flow Conditions

	column 1	column 2
30 cm	5.74 ± 0.24	3.77 ± 0.25
60 cm	5.52 ± 0.28	3.83 ± 0.17
90 cm	5.77 ± 0.22	3.17 ± 0.22
120 cm	5.12 ± 0.12	3.35 ± 0.29
average	5.46 ± 0.15	3.53 ± 0.16

similar at all sampling ports (Table 5). This confirms that the diesel fuel was homogeneously distributed. The measured average ^{222}Rn activity in water from column 2 (3.53 ± 0.16 kBq m^{-3}; Table 5) corresponded to the expected ^{222}Rn activity in water from column 2 (3.38 ± 0.18 kBq m^{-3}). The expected activity was based on the measured diesel fuel saturation *S* in column 2, the diesel fuel−water partition coefficient *K* from the batch experiment, and the average ^{222}Rn activity at no flow conditions in column 1 using the linear relation between $A_e^{S=0}/A_e^{S>0}$ and *S*. This relationship was derived in the theory section (eq 8) and verified in the batch experiments (Figure 2).

Column Experiment/Flow Conditions. At flow conditions, the ^{222}Rn activity in the water phase increased in the uncontaminated column 1 with increasing column length or residence time (Figure 3). In the contaminated column 2, the ^{222}Rn activity in water samples decreased with increasing column length (Figure 3). To evaluate whether the observed ^{222}Rn activities in the water phase approached the no flow ^{222}Rn activities as predicted by the model, the expected ^{222}Rn activities were calculated using eq 9. The parameters required in eq 9 were obtained as follows: the diesel fuel−water partition coefficient *K* was taken from the batch experiment, *S* corresponded to the measured diesel fuel saturation, and $A_e^{S=0}$ and $A_e^{S>0}$ corresponded to the average ^{222}Rn activity measured at no flow conditions in columns 1 and 2, respectively. In both columns, the measured ^{222}Rn activities agreed with the predicted values (Figure 3). In column 2, at 60, 90, and 120 cm, the deviation between the ^{222}Rn activities at flow conditions and the ^{222}Rn activities at no flow conditions was within the range of uncertainty of the measurement. This suggests that a residence time in the contaminated zone of at least 6.4 days (sampling port at 60 cm) is required before measured aqueous ^{222}Rn activities can be used to estimate the diesel fuel saturation using eq 8.

To evaluate the accuracy of the ^{222}Rn method in determining NAPL saturation, the diesel fuel saturation in column 2 was calculated using the linear relation between $A_e^{S=0}/A_e^{S>0}$ and *S* that was derived in the theory section (eq 8) and verified in the batch experiments. For $A_e^{S>0}$, the average of the ^{222}Rn activities measured in column 2 at 60, 90, and 120 cm at flow conditions was taken (3.43 ± 0.20 kBq m^{-3}). For $A_e^{S=0}$, the ^{222}Rn activity measured at flow conditions in column 1 at 120 cm (4.9 ± 0.32 kBq m^{-3}) was used. The diesel fuel−water partition coefficient *K* was taken from the batch experiment. From these values, the calculated diesel fuel saturation was 1.0 ± 0.28%, which is slightly lower than the measured diesel fuel saturation (1.4 ± 0.06; Table 3). The deviation between the calculated and the measured diesel fuel saturation was due to the fact that $A_e^{S=0}$ was not reached in column 1 (Figure 3). If the average no flow ^{222}Rn activity in column 1 was used for $A_e^{S=0}$, a diesel fuel saturation of 1.4 ± 0.17% would be obtained that corresponded to the measured diesel fuel saturation.

^{222}Rn Activities at the Field Site. At the field site, groundwater samples were taken three times at natural gradient flow conditions to determine the ^{222}Rn activities. The ^{222}Rn activities measured in the monitoring wells KB2, KB8, and KB9 were assumed to represent $A_e^{S=0}$ (Table 6). A

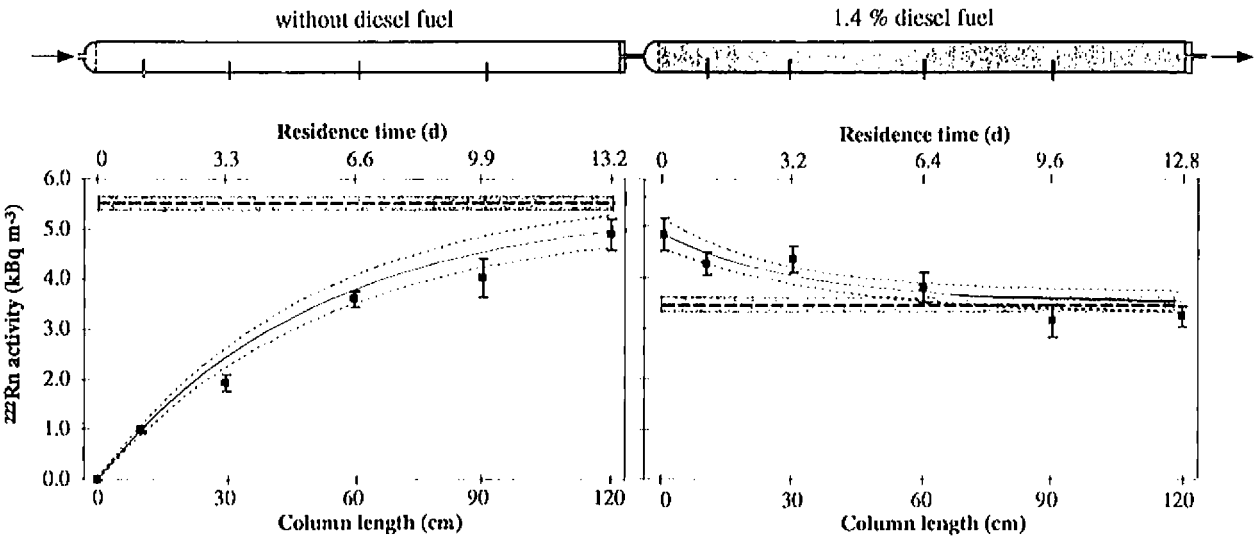

FIGURE 3. Schematic illustration of the columns (operated in upright position). ^{222}Rn activities in water samples from column 1 (uncontaminated) and column 2 (contaminated with diesel fuel) after 8 weeks of steady flow (■). (—) ^{222}Rn activities calculated based on the average ^{222}Rn activities at no flow conditions and the average diesel fuel saturation using eq 9. (- - -) Range of standard uncertainty of the calculated ^{222}Rn activity. (— —) Average ^{222}Rn activity at no flow conditions. (Hatched area) Range of standard uncertainty of the average ^{222}Rn activity at no flow conditions.

TABLE 6. ^{222}Rn Activities and Concentrations of Dissolved Hydrocarbons Measured in Water Samples from Monitoring Wells of the Field Site in Menziken

	^{222}Rn activity[a] (kBq m^{-3})			dissolved hydrocarbons[b] (mg L^{-1})
well	**9/12/94**	**10/18/95**	**10/29/96**	**10/18/95**
Upgradient of Initially Contaminated Zone				
KB2	6.0	7.5	9.0	<0.01
KB8	–[c]	9.4	9.8	<0.01
KB9	6.9	7.8	10.1	–
average[d]	6.5	8.2	9.6	
In Initially Contaminated Zone				
KB7	**4.7**	**4.4**	**6.1**	0.35
S6	**3.7**	**4.7**	**5.2**	0.20
S7	**2.2**	**5.7**	**6.0**	0.01
S8	**4.2**	**5.2**	–	0.10
KB1	5.7	6.9	**7.7**	0.21
KB3	5.2	**6.4**	**8.0**	0.04
KB10	–	8.6	10.9	<0.01
KB12	–	9.2	10.1	<0.01
KB15	**4.5**	8.8	9.5	<0.01
Outside but Not Upgradient of Initially Contaminated Zone				
KB5	7.7	10.5	12.2	–
KB11	–	9.2	8.7	–
KB14	–	9.5	11.4	<0.01

[a] Standard uncertainty of ^{222}Rn activity measurement: ±20% on 12/9/94 and 10/18/95 and ±10% on 10/29/96. ^{222}Rn activities significantly smaller than average of ^{222}Rn activities measured at wells KB2, KB8, and KB9 ($A_e^{S=0}$) are printed in bold. [b] Standard uncertainty of measurement of dissolved hydrocarbon concentration: ±20%. [c] –, not measured. [d] Average of ^{222}Rn activities measured at wells KB2, KB8 and KB9.

regional flow model indicated that the groundwater was in the aquifer for more than 20 days before these wells were reached (unpublished data), and the wells are situated upgradient of the diesel fuel-contaminated zone. ^{222}Rn activities significantly smaller than the average value of the wells KB2, KB8, and KB9 are referred to as ^{222}Rn deficits (Table 6).

In the monitoring wells KB7, S6, S7, and S8, a ^{222}Rn deficit was observed at all sampling days (Table 6). In the wells KB1, KB3, and KB15, a ^{222}Rn deficit was observed only at one or two sampling days (Table 6). ^{222}Rn deficits were only found in monitoring wells within the zone that was initially contaminated with non-aqueous-phase diesel fuel. However, the extension of the initially contaminated zone did not necessarily correspond to the extension of the contaminated zone at the time of the ^{222}Rn activity measurements. To establish the correlation between the ^{222}Rn deficits and the presence of diesel fuel, dissolved hydrocarbon concentrations were measured on October 18, 1995. Except for KB1, all monitoring wells that contained dissolved hydrocarbons above the detection limits showed a ^{222}Rn deficit (Figure 4). This provides further evidence that the ^{222}Rn deficit was due to the presence of the diesel fuel. However, there is no quantitative correlation between dissolved diesel fuel and the diesel fuel saturation.

Estimation of the Diesel Fuel Saturation. The ^{222}Rn activities measured in groundwater samples from the wells KB7, S6, S7, and S8 were used to estimate the remaining diesel fuel saturation from the location of the former tank to the wells of cross section B–B′ (Figure 1) after the end of the in situ bioremediation. The values measured in 1994 were not included in the calculation because the in situ bioremediation was re-implemented between October 1994 and May 1995. The diesel fuel saturation was estimated using the linear relation between $A_e^{S=0}/A_e^{S>0}$, and the diesel fuel saturation S (eq 8). $A_e^{S=0}$ was assumed to correspond to the average of the ^{222}Rn activities measured in groundwater from the wells KB2, KB8, and KB9. The value for K was taken from the batch experiment. The ratio $A_e^{S=0}/A_e^{S>0}$ was between 1.45 and 1.86 for the wells KB7, S6, S7, and S8 in 1995 and 1996 with an average value of 1.67 ± 0.15 (n = 7). On the basis of this value, an average diesel fuel saturation of 1.5 ± 0.35% was obtained. The calculated value is in the range of the value measured in an aquifer sample excavated from the contaminated zone in November 1992, when a diesel fuel saturation of S = 1.9% was found (*24*). However, in 1992, aquifer material was excavated only at one location.

The diesel fuel saturation that was calculated based on the ^{222}Rn activities in groundwater has to be considered as a rough estimation of the actual diesel fuel saturation for several reasons:

(1) In aquifers, diesel fuel and other NAPLs are usually heterogeneously distributed while the equation used to calculate the diesel fuel saturation relies on the assumption of a homogeneous NAPL distribution. Furthermore, the

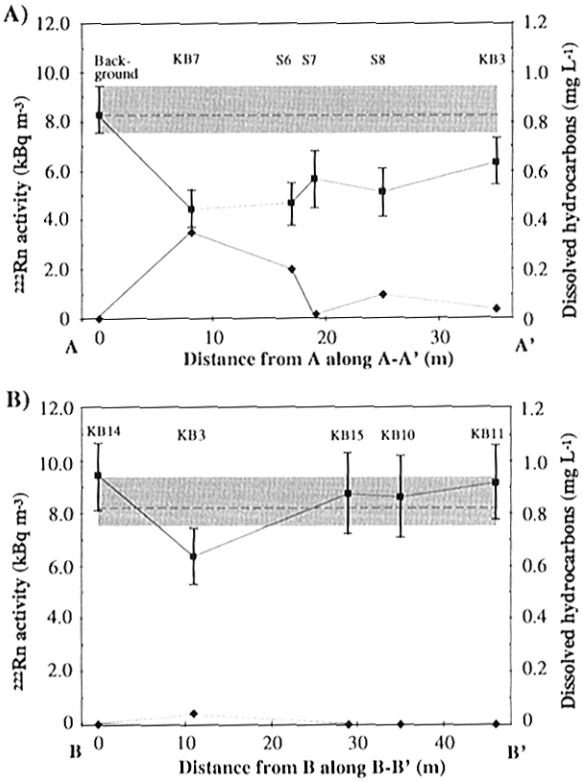

FIGURE 4. ^{222}Rn activities (■) and dissolved hydrocarbon concentrations (♦) measured on October 18, 1995, in groundwater from monitoring wells; (A) along the cross section A−A′; (B) along the cross section B−B′. (− −) Average of ^{222}Rn activities measured on October 18, 1995, in wells KB2, KB8, and KB9 (= background). (Hatched area) Range between highest and lowest ^{222}Rn activity measured in these three wells.

laboratory experiments made to verify the equations were performed using a homogeneous diesel fuel saturation.

(2) Mixing of groundwater from the contaminated zone with groundwater from the uncontaminated zone can lead to an increase of the ^{222}Rn activity in the groundwater sample and thus to a lower calculated NAPL saturation (eq 8).

(3) If the residence time of the groundwater in the contaminated zone is low, the emanation−decay steady-state ^{222}Rn activity may not be reached (see column experiment). If the emanation−decay steady-state is not reached in the contaminated zone, the NAPL is underestimated when calculated using eq 8.

Further investigations will focus on the effect of these three factors on ^{222}Rn activities in the field and thus on the calculated diesel fuel saturation.

Comparison of ^{222}Rn with Artificial Partitioning Tracers. Compared to artificially injected partitioning tracers, ^{222}Rn has an advantage to be naturally present in aquifers, whereas the addition of an artificial tracer to a large groundwater volume requires an expensive groundwater injection scheme. To quantify the NAPL saturation, ^{222}Rn activities need to be measured, in principle, only once, while the use of artificial tracers requires many measurements to obtain complete breakthrough curves (*2*, *6*). To use ^{222}Rn as a partitioning tracer, the ^{222}Rn emanation rate must be constant in the aquifer. This can be verified by measuring ^{222}Rn activities in the water phase at several locations in the uncontaminated zone. Similarly to other partitioning tracers, ^{222}Rn reflects the NAPL saturation along flow paths of the groundwater and not necessarily the average saturation in a given volume of the aquifer. Variations of the hydraulic conductivity due to variations of the geological structure or due to the presence of NAPL at a high saturation may cause the groundwater to bypass the NAPL-contaminated zone. This may lead to an underestimation of the actual NAPL saturation (*6*). In addition, mass transfer limitations may cause an underestimation of the NAPL saturation (*6*). When using ^{222}Rn as a partitioning tracer, the diesel fuel saturation close to the monitoring well is weighted more strongly than the NAPL saturation further away since ^{222}Rn activities re-equilibrate in response to changing NAPL saturation. Furthermore, ^{222}Rn activities increase again once the groundwater has left the zone of NAPL contamination. Therefore, monitoring wells used to determine ^{222}Rn activities should be located close to or within the NAPL-contaminated zone.

Acknowledgments

The authors thank G. Wyssling, A. Stöckli, W. Jucker, and Ch. Herzog for cooperation at the field site, H. R. Zweifel for analyzing samples, and K. Häberli and W. Kinzelbach for stimulating discussions. The manuscript was significantly improved through reviews by G. T. Townsend and four unknown referees. The work was supported by the Swiss National Science Foundation (Priority Programme Environment).

Literature Cited

(1) Mayer, A. S.; Miller, C. T. *J. Contam. Hydrol.* **1992**, *11*, 189−213.
(2) Jin, M.; Delshad, M.; Dwarakanath, V.; McKinney, D. C.; Pope, G. A.; Sepehrnoori, K.; Tilburg, C. E.; Jackson, R. E. *Water Resour. Res.* **1995**, *31*, 1201−1211.
(3) Tang, J. S.; Harker, B. *J. Can. Pet. Technol.* **1991**, *30*, 76−85.
(4) Tang, J. S.; Harker, B. *J. Can. Pet. Technol.* **1991**, *30*, 34−42.
(5) Wilson, R. D.; Mackay, D. M. *Environ. Sci.Technol.* **1995**, *29*, 1255−1258.
(6) Nelson, N. T.; Brusseau, M. L. *Environ. Sci.Technol.* **1996**, *30*, 2859−2863.
(7) Horiuchi, K.; Murakami, Y. *Int. J. Appl. Radiat. Isot.* **1981**, *32*, 291−294.
(8) Surbeck, H. *Nucl. Tracks Radiat. Meas.* **1993**, *22*, 463−468.
(9) Wong, C. S.; Chin, Y.-P.; Gschwend, P. M. *Geochim. Cosmochim. Acta* **1992**, *56*, 3923−3932.
(10) Andrews, J. N.; Wood, D. F. *Trans. Inst. Min. Metall.* **1972**, *81*, 198−209.
(11) Rama. *Curr. Sci.* **1991**, *61*, 751−755.
(12) Krishnaswami, S.; Seidemann, D. E. *Geochim. Cosmochim. Acta* **1988**, *52*, 655−658.
(13) Maraziotis, E. A. *Environ. Sci. Technol.* **1996**, *30*, 2441−2448.
(14) Hoehn, E.; von Gunten, H. R. *Water Resour. Res.* **1989**, *25*, 1795−1803.
(15) Hoehn, E.; von Gunten, H. R.; Stauffer, F.; Dracos, T. *Environ. Sci. Technol.* **1992**, *26*, 734−738.
(16) Brusseau, M. L. *Water Resour. Res.* **1992**, *28*, 33−45.
(17) Van Genuchten, M. T.; Alves, W. J. U.S. Department of Agriculture, Technical Bulletin No. 1661; Washington, DC, 1982.
(18) Leo, A.; Hansch, C.; Elkins, D. *Chem. Rev.* **1971**, *71*, 525−553.
(19) Mercer, J. W.; Cohen, R. M. *J. Contam. Hydrol.* **1990**, *6*, 107−163.
(20) Toride, N.; Leij, F. J.; van Genuchten, M. T. U.S. Salinity Laboratory, Agricultural Research Service, Research Report No. 137. U.S. Salinity Laboratory: Riverside, CA, 1995.
(21) Schwarzenbach, R. P.; Westall, J. *Environ. Sci. Technol.* **1981**, *15*, 1360−1366.
(22) Hunkeler, D.; Höhener, P.; Häner, A.; Bregnard, T. P.-A.; Zeyer, J. Quantification of hydrocarbon mineralization in a diesel fuel-contaminated aquifer treated by *in situ*−biorestoration. *Groundwater Quality: Remediation and Protection*; IAHS Publication No. 225; IAHS Press: Wallingford, Oxfordshire, 1995; pp 421−430.
(23) Hunkeler, D.; Höhener, P.; Bernasconi, S.; Zeyer, J. *Water Ressour. Res.* Submitted for publication.
(24) Bregnard, T. P.-A.; Höhener, P.; Häner, A.; Zeyer, J. *Environ. Toxicol. Chem.* **1996**, *15*, 299−307.

(25) International Organization for Standardization. *Guide to the expression of uncertainty in measurement*; International Organization for Standardization: Geneva, 1993.
(26) Zar, J. H. *Biostatistical analysis*; Prentice-Hall: Englewood Cliffs, NJ, 1984.